Numerical Study of the Behaviour of Embankment Constructed over Soft Soil Stabilized with Ordinary and Geosynthetic - Reinforced Stone Columns

Mohamed Khodary [1]
Mahmoud M. Abu Zeid[2]
Mostafa A. Abdel-Naiem [3]

Abstract

Structures constructed on soft soils may undergo significant settlement, local or global instability, and a significant lateral displacement of the soft soil layer. Ordinary stone columns (OSC) and stone columns strengthened with geosynthetic reinforcement reduce settlement and improve the subsoil's bearing capacity. Numerical analyses have been performed using a 3-dimensional finite element program (PLAXIS3D) to investigate the time-dependent behavior of embankments resting on stone columns constructed in very soft clay. The geosynthetic encasement is the more typical type of reinforcement; however, laminated layers can be adopted in this study. The geosynthetics material was used to strengthen the OSC in the form of vertical encasement, horizontal stripes, and combined vertical-horizontal reinforcement and vertical-basal geogrid reinforcement (BGR). This research compares these forms of reinforcement on embankment behavior. The research results showed that using the encased stone column (ESC) and the vertical-horizontal reinforced stone columns (V-HRSC) have provided a considerable improvement in the lateral deformation of the column over its length, generation, and dissipation of excess pore pressure, and settlement. An increase in factor of safety (FOS) against failure of the embankment was observed by 53% using the ESC compared to untreated soil. Using the horizontal geosynthetic layer (HGL) and the (BGR) after encasing the stone columns has no effect on the safety factor as the failure mechanism converted from deep-seated to surface failure.

1. Introduction

Because of the lack of appropriate construction sites because of fast urbanization and industrial expansion, the demand for construction in abandoned sites is growing day by day. When constructing embankments or structures on a soft soil deposit, geotechnical engineers may face difficult challenges. Some of the key issues are substantial lateral deformation, local or global slope instability,

[1] *M.Sc. Researcher, Civil Engineering Department, Faculty of Engineering, South Valley University, Egypt.*
   eng.mohamedkhodary@eng.svu.edu.eg -

[2] *Lecturer, Civil Engineering Department, Faculty of Engineering, South Valley University, Egypt.* eng_abuzeid@yahoo.com

[3] *Professor of Engineering and Geotechnical Foundation, Faculty of Engineering, Assiut University, Egypt.*
   Mostafaabdo@aun.edu.eg

excessive settlements, and deep-seated embankment failure. Soft soils must be improved to mitigate these issues to enhance the engineering characteristics of this foundation soil. Appropriate soil improvement methods including sand compacted columns, deep mixed columns, and stone columns were suggested. Stone columns are an environmentally friendly cost-effective and widely used type of ground improvement for different types of structures including embankments and buildings **[1-5]**. Using stone columns below the embankments prevents excessive settlement, enhances stability, increases the load-carrying capacity of the weak foundation soil, speeds up the consolidation process, and reduces the risk of liquefaction **[2, 4, 6-8]**.

The stone column method does not work effectively when the in-situ soil cannot provide appropriate lateral confinement. The issues mentioned are attributed to the penetration of the column's aggregate into weak soil, low drainage because of clogging of aggregate and poor performance during shear stress. In such cases encasing the stone columns with geosynthetic tubes composed of geotextiles or geogrids can increase its performance. The geosynthetic reinforcement serves as a safety cover for the stone columns material resulting in increased load carrying capacity and efficient pore pressure dissipation. To investigate the failure mechanism of stone column supported embankments, an experimental, two and three-dimensional numerical modelling has been conducted by Chen et al **[9]**. They concluded that under the embankment loading the most common failure mode in the encased stone columns is bending failure rather than shear, column's bending occurred because of the embankment and the subsoil Sliding as well as unequal lateral loading acting on the columns. The most typical failure mechanism for sand compacted and stone columns are shear failure **[10]**. **Figure 1** indicates the different types of probable embankment slope failures. In recent years many numerical studies conducted for studying the slope stability of embankments constructed over stone columns strengthened soft soil (for example,**[3, 8, 11-17]**).

This paper aims to investigate numerically using the finite element code, PLAXIS 3D 2020, the performance of a full-scale embankment constructed on soft soil strengthen with deferent methods (i.e., ordinary stone column (OSC), Horizontally Reinforced Stone Columns (HRSC), Encased Stone Columns (ESC), combined Vertical-Horizontal Reinforced Stone Columns (V-HRSC), and ESC in combination with Basal Geogrids reinforcement (BGR)). The effect of the methods on settlement mitigation, creation and dissipation of excess pore pressure, lateral column deformation over its length, embankment stability, and the stress concentration ratio is assessed under embankment loading.
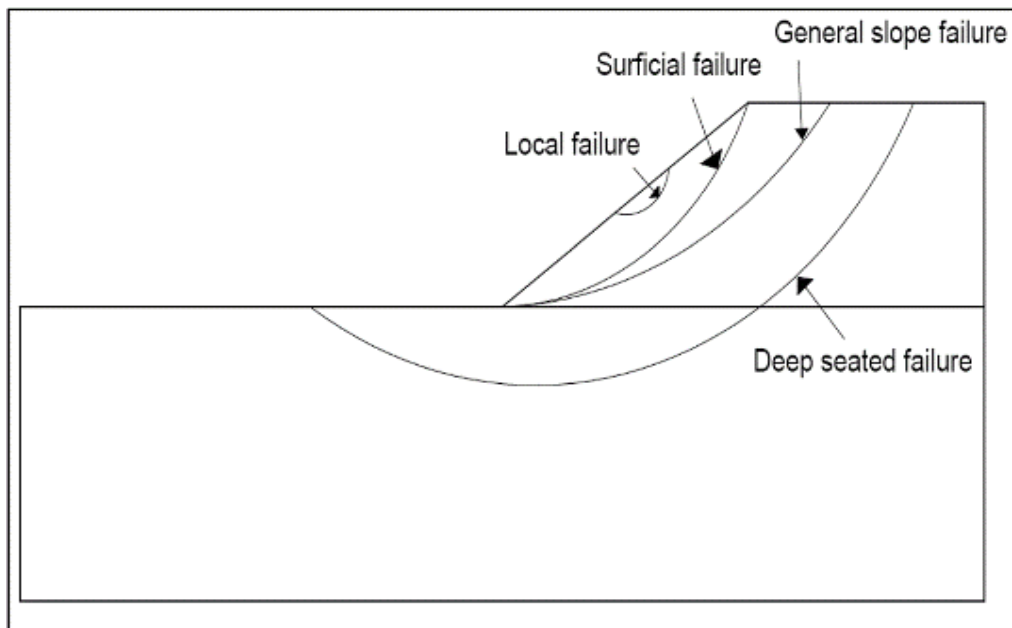
Figure 1. Potential slope stability failures [18].

2. Description of the Reference Case

It is predicted that the first step of the numerical simulations will be to ensure the numerical model's reliability, therefore the numerical modelling in this study was based on a well-documented case of an embankment constructed on soft soil explained in the PLAXIS 3D manual. This model was selected as the reference case for the numerical modelling in this study and validated with the baseline case explained in this manual **[19]**.

2.1. General description

Figure 2 represents the cross-section geometry of the embankment employed in this investigation. The embankment is 40 m wide, 4 m high, and has a 1:3 side slope. The embankment was built on a 6 m thick layer of soft soil (3m peat layer and 3m clay layer). A 4 m thick layer of dense sand fills up the bottom layer. Due to the embankment's axial symmetry around its center and to speed up computational operations, only half of the embankment was modeled. The embankment was built in 33 days for the comparative study. The behavior of the embankment was investigated both during construction and in the post-construction period. The embankment was constructed in 2 m increments, in two stages, each stage followed by a consolidation period.

2.2. Geosynthetic-Encased Stone Columns

Stone columns with a diameter of 0.8 m and a length of 6 m were employed in this study. The stone columns were arranged in a square grid pattern with a center to center spacing of 2m. Full geosynthetics encasement was assumed for the encased stone columns, the geosynthetics axial stiffness was $J_{enc} = 1000$ kN/m. The basal geogrid used under the embankment material and horizontal geosynthetic layer has an axial stiffness of $J_{bas} = 2000$ kN/m, $J_{HGL} = 2000$ kN/m respectively. The groundwater table was set to be 1.0 m under the peat layer's surface.
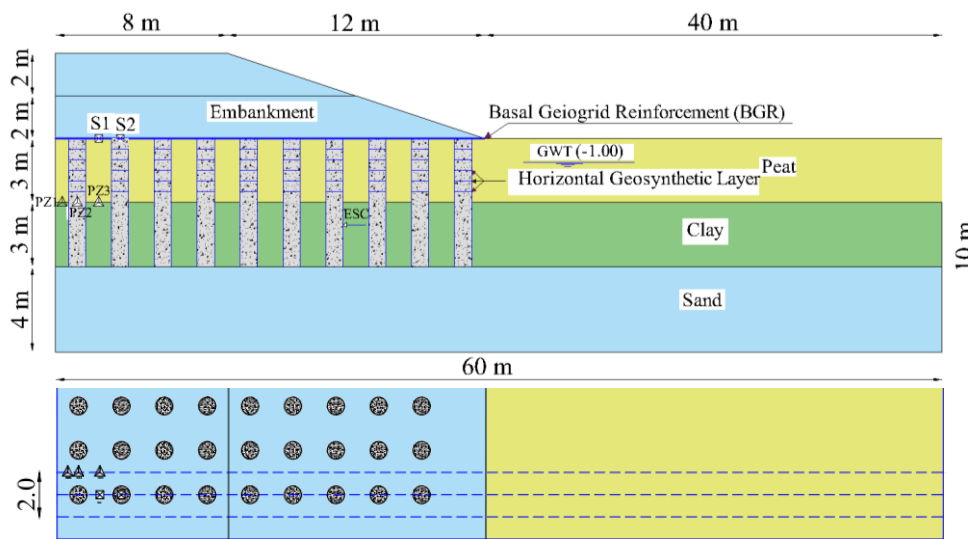
Figure 2 . Embankment cross-section and instrumental layout for numerical modeling

3. Numerical Model

In the current study, the finite element program PLAXIS 3D was used to perform the 3D numerical analysis, Because of its ability to perform time-dependent problems [20]. PLAXIS 3D is a three-

dimensional finite element program designed specifically for geotechnical problem analysis **[11, 13, 14, 21]**.

3.1. Model configuration

A 3D rectangular slice unit is usually used to simulate column-supported embankments because of the symmetrical conditions. Several researchers **[7, 8, 22]** have been successfully used the three-dimensional slice with a width equal to half the column center to center spacing. Due to the simplicity of generating mesh and collection of computational outputs, especially the force generated in the column, the three-dimensional slice with a width equal to a whole column center to center spacing had also been extensively employed to analyze the behavior of a stone columns system (i.e., **[3, 9, 11-13, 21, 23, 24]**). The slice adopted in this study was 2m-wide as shown in **Figure 3**. The 10-node tetrahedral elements have been used in PLAXIS 3D to simulate the soil volume to give a good representation of soft soil layers, stone columns, and embankment material. The tetrahedral elements with 10-nodes are formed during the process of generating the 3D mesh. This variety of elements provides a second-order displacement relationship while keeping linear pore water pressure development **[20]**. The geotextile (i.e., encasement, horizontal layer) and the basal geogrid element were modeled as an isotropic nonlinear geogrid element in PLAXIS 3D, consisting of 6-node triangular surface elements having 3- translational degrees of freedom for each node. Geogrids are slender structures with axial stiffness but with no bending stiffness. Geogrids can only sustain tensile forces and no compression. Basically, these objects are employed to represent soil reinforcements. Stone columns generally collapse due to radial bulging rather than shear failure. Also, the Installation effect of stone columns automatically causes the formation of an undulating interface. Furthermore, the soil-stone columns interface is a heterogeneous zone, with different shear strength values depending on the sand column installation method **[25-27]**. As a result, no interface element is assigned between the stone columns and the adjacent soil in the current study. Also, the interface between the basal geogrid and embankment fill soil was not considered in the analysis assuming full bonding between them (i.e., no allowed relative movement at the contact surface). This assumption was argued to have little influence on geogrid results because pullout tests revealed that slip took place in the soil mass rather than at the interface between soil and geogrid in many soils unless the confining stress is extremely small [28, 29]. To ensure reducing the boundary effect, the adopted model boundary dimensions were 2 m in the y-direction, 60 m in the x-direction, and 10 m in the z-direction from the ground level. Regarding the model's displacement boundary conditions, it was only allowed to deform horizontally in the vertical plane (i.e., roller boundaries), whereas the bottom boundary has been restricted in all three dimensions. For the outflow boundary conditions, the groundwater was 1.0 m below the ground surface. The upper and lower boundaries, as well as the boundary of flow condition at x=60, were defined to be permeable, while the other boundaries were fully impermeable.

The current analysis's first calculation phase was to generate the initial stress condition and pore pressures using the "at-rest" lateral earth pressure (coefficient of at-rest earth pressure K0 calculation type) method. Consequently, the installation effects of the stone column were ignored, according to the fact that the embankment is constructed four years after the column's installation. The current construction phase of the modeled embankment was used to simulate the load application, accompanied by an appropriate consolidation period. The calculation steps are comprised of the cluster's activating that is related to the different strata of the embankment. Dissipation of time-dependent excess pore water pressures in the saturated soft ground layers was analyzed by defining a consolidation period between the stages of construction. The consolidation period, in general, is the required consolidation time that can achieve a certain soil strength and stiffness, satisfying both bearing capacity and settlement design criteria, it can be calculated from the back analysis method which is applied to attain a minimum required degree of consolidation or a stabilized case for

settlement or till the minimum excess pore pressures condition is reached which usually taken equal to 1.0 kPa [30, 31]. In this study, the consolidation period after the first and second construction stages was calculated from a back analysis to achieve a minimum excess pore pressure value of 1.00 kPa. Details of building construction stages in the conducted FE analysis are tabulated in **Table 1**.
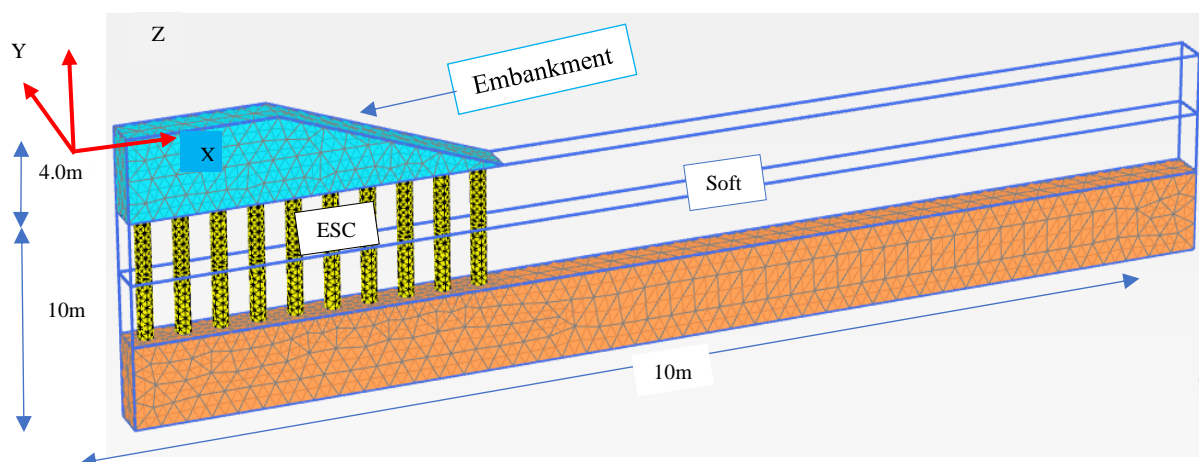
Figure 3. Three-dimensional finite element mesh

Table 1: The phases of construction in the finite-element analysis

phase	Calculation Type	Description
Initial phase	K0 procedure	Generation of the initial stresses (K0 – condition)
Phase 1	Consolidation	2-meter-high embankment execution
Phase 2	Consolidation	
Phase 3	Consolidation	2-meter-high embankment execution
Phase 4	Consolidation	the calculation is continued until the minimum excess pore pressure (1 kPa) condition is reached
Phase 5	Safety	Safety factor calculation using (phi/c reduction) method

Several advanced constitutive models that accurately simulate the soil behavior, including the Hardening Soil (HS) model, Linear Elastic Perfectly Plastic Model (Mohr-Coulomb Model), and the Soft Soil (SS) model, were presented in various research. The HS model was used to simulate the embankment and the sand layers properties as it's suitable for evaluating important properties of fine and coarse soils since it considers the stress dependence of stiffness parameters as well as volumetric stiffness and shear dilatancy properties [32]. The soft soil model was used to simulate the soft clay and peat layer. The parameters of the Soft Soil model include compression (λ^*) and swelling (κ^*) indices in addition to strength parameters, which are calculated using the known formulas $\kappa^* = 2C_c/2.3 (1 + e_0)$ and $\lambda^* = C_c/2.3 (1 + e_0)$ based on a one-dimensional compression test. The stone column material was modeled using Mohr-Coulomb Model (MCM) with Young's modulus (E) equal to the secant modulus at 50% strength, denoted as E50 which is a suitable stiffness parameter in many problems [33]. The properties of Embankment, Sand, Peat, and Clay material that was taken from the PLAXIS 3D tutorial **[19]**, in addition to Stone columns properties are tabulated in **Table 2**.

Table 2: Material properties

Parameter	Embankment	Sand	Peat	Clay	Stone columns
Material model	Hardening Soil	Hardening Soil	Soft Soil model	Soft Soil model	Mohr-Coulomb
Drainage type	Drained	Drained	Undrained (A)	Undrained (A)	Drained
Soil unit weight above phreatic level γ_{unsat} (kN/m3)	16	17	8	15	19
Soil unit weight below phreatic level γ_{unsat} (kN/m3)	19	20	12	18	20
Initial void ratio e_{int}	0.5	0.5	2.0	1.0	0.5
Modified compression index $\lambda*$	-	-	0.15	0.05	-
Modified swelling index ($\kappa*$)	-	-	0.03	0.01	-
Secant stiffness E_{50}^{ref} (kN/m2)	$2.5*10^4$	$3.5*10^4$	-	-	
Young's modulus (E) for MCM	-	-	-	-	$3.5*10^4$
Poisson's ratio ν	-	-	-	-	0.3
Tangential stiffne E_{oed}^{ref} (kN/m2)	$2.5*10^4$	$3.5*10^4$	-	-	
Unloading and reloading stiffness, E_{ur}^{ref} (kN/m2)	$7.5*10^4$	$1.05*10^5$	-	-	
Power for stress-level dependency of stiffness) m)	0.5	0.5	-	-	-
Cohesion (constant) C_{ref} (kN/m2)	1.0	0.0	2.0	1.0	1.00
Friction angle φ'	30	33	23	25	35
Dilatancy angle ψ	0.0	3.0	0	،	5.0
Horizontal permeability (x-direction) K_{HZ} (m/day)	3.499	7.128	0.1	$47.52*10^{-3}$	10.37
Vertical permeability K_V (m/day)	3.499	7.128	0.05	$47.52*10^{-3}$	10.37
Change in permeability Ck	$1*10^{15}$	$1*10^{15}$	1.0	0.2	$1*10^{15}$
Over-consolidation ratio	1.0	1.0	1.0	1.0	-
Pre-overburden pressure	0.0	0.0	5.0	0.0	-

4. Safety analysis

In PLAXIS 3D, the Safety analysis type can be used to calculate the global factor of safety (FOS). The shear strength parameters of the soil, **tan Ø** and **c**, and the tensile strength are gradually reduced in the Safety calculations until the structure fails. The above-mentioned technique is called the **phi/c** reduction technique. The total multiplier directly controls the reduction of the strength parameters (**S**Msf). In the analysis, this parameter is constantly updated until it reaches the limit state. As a result, the safety factor may be effectively determined by plotting the oscillation of the Total Multiplier (**S**Msf) against Total deformation (Δu).

5. Parametric Studies

Different parameters were used to study the performance of soft soil strengthened with stone columns. In the current numerical modeling, six different scenarios were considered.
(a) Soft soil with no treatment technique.
(b) Ordinary stone columns (OSC).
(c) Horizontally Reinforced Stone Columns (HRSC).
(d) Geosynthetic encased stone columns (ESC).
(e) Combined vertical-horizontal reinforced stone columns (V-HRSC).
(f) ESC in addition to Basal Geogrids reinforcement (BGR).
At first, the embankment loading was applied on the untreated soft soil and the behavior of the embankment during construction and monitoring time was studied. The OSC was installed in the second scenario by displacing an equivalent amount of the unreinforced soil, and the construction of the embankment was modeled. For the third stage, an appropriate geogrid layer was placed inside the OSC (i.e., HRSC). In the fourth case, effective geosynthetic reinforcement was wrapped around the stone column over its length and its performance was investigated. In the five cases, horizontal geosynthetic layers were placed into the ESC over a certain length of the column (about 60% of the stone column's length). Finally, the embankment behavior was studied when Basal Geogrids reinforcement (BGR) was placed over the ESC on the ground surface.

6. Numerical results and Comparisons

6.1. Settlement analysis

The time-settlement curves were used to investigate the performance of the Treated soft clay using stone columns. Surface settlement induced by embankment weight was studied at various periods. **Figure 4** depicts the time settlement response at the observation point **S1** located under the embankment at the midpoint between stone columns. It has been observed that without any ground improvement, Soil settlement was higher than its value when using the stone columns in native soil. **Figure 4** demonstrates that the stone column significantly minimizes the settlement induced by embankment loading, the reduction of settlement was observed to be 24.3 % from its value when no improvement was used, this value increased to nearly 51.5 % when using the HRSC this indicates the effectiveness of horizontal layers in reducing lateral bulging of the stone columns and increasing its stiffness. The use of geosynthetic encasement in stone columns minimizes settlement even more. The confining stress increases as the stiffness increases, resulting in higher load-carrying capacity. According to **Figure 4** encased stone columns eliminate settlement by 60% compared to unimproved soil. The settlement reduction presents a continued decrease when using BGR over ESC and the (H-VRSC) to 63% and 68%, respectively. **Figure 4b** illustrates the time-dependent variation of settlements on the column's surface and the adjacent soil surface. The surface settlements, both on the column's surface and in the adjacent soils, increased rapidly during the construction stage and then gradually attain stable values throughout the consolidation stage. The settlement on the top of the columns was less than the surrounding soil settlement, this was due to the higher stiffness of the granular material. The settlement profile below the embankment at the end of the observation period for the different improvement methods was studied. As demonstrated in **Figure 5** the maximum value of the surface settlement was under the embankment center. The surface settlement decrease towards the embankment toe. The extreme settlement values were in the case of soil without improvement this value was mitigated using the stone columns improvement method. The minimum settlement occurs when using the encased stone columns combined with the horizontal geosynthetics layer (i.e., H-VRSC).

(a) at point S1   (b)
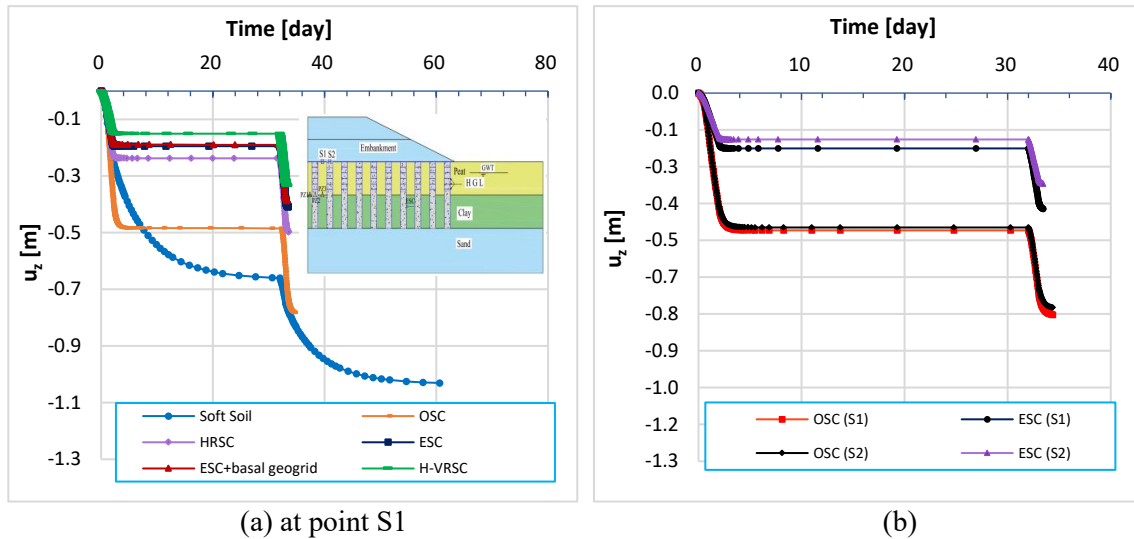
Figure 4 . (a) Settlements at a midpoint between stone columns versus time. (b) Settlements over the stone column's head and the surrounding soil versus time
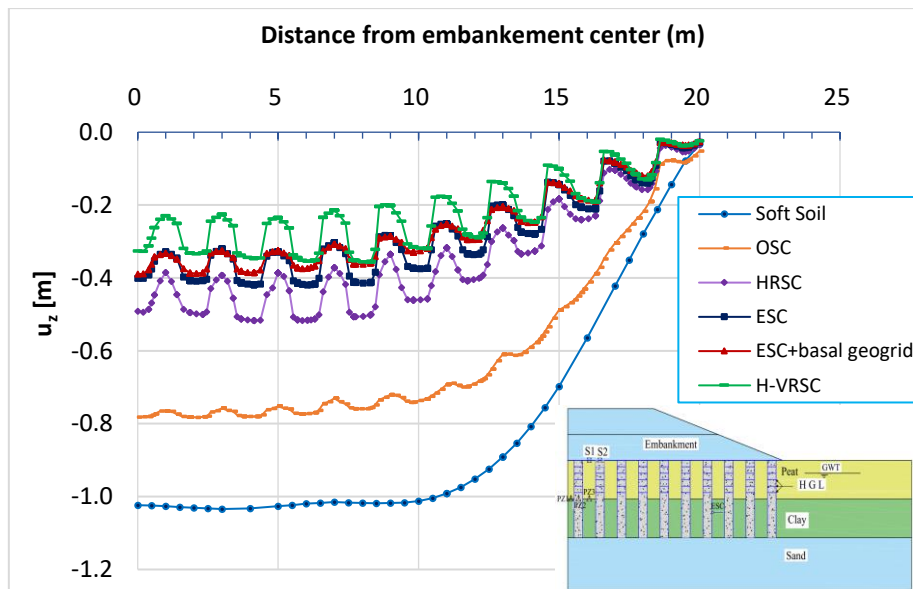
Figure 5 . Settlement profile below the embankment at the end of monitoring time

Studying horizontal displacements of foundation soil caused by embankment load during construction is important, especially for structures close to the embankment, including cables, pipelines, and piles **[34]**. These horizontal deformations impose extra pressures and moments on neighboring structures, potentially destroying the foundation and the structure above it **[35]**. **Figure 6** shows the effect of the adopted improvement methods on maximum horizontal deformations below embankment toes at the end of monitoring time. As shown in **Figure 6** the maximum horizontal displacement (i.e., 20 cm) is produced by unimproved soil. This value was reduced to a value of 8cm, 4cm, 2.9cm, and 3cm with a reduction percentage of 60%,80%,85.5%, and 85% compared to the unimproved soil when using the OSC, HRSC, ESC, V-HRSC, respectively.

The minimum value was observed in the case of ESC with BGR with a reduction of 95%. Consequently, it could be concluded that using the BGR under the embankment supported by the ESC enhances its stability and minimizes the value of the external lateral loads imposed on the adjacent structures.
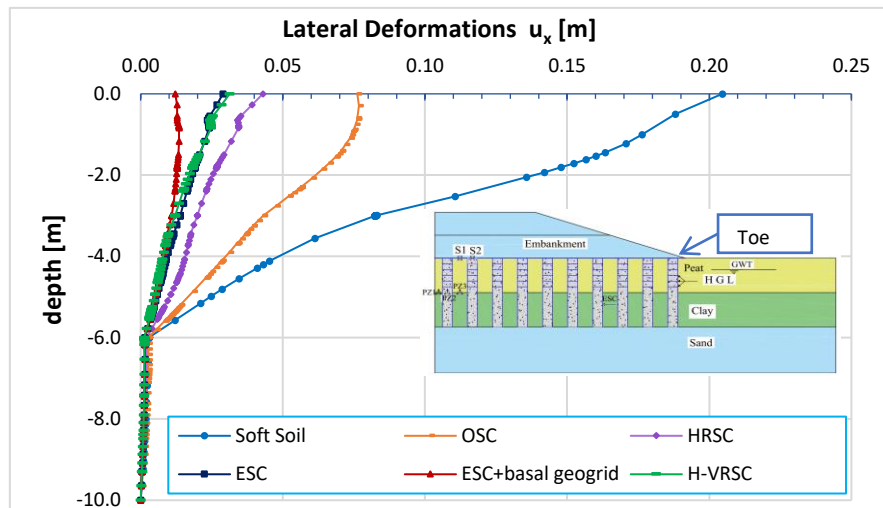
Figure 6. Horizontal displacements below the embankment toes at the end of the monitoring time

6.2. Factor of safety

Safety analysis has been conducted using the **phi/c** reduction technique to investigate the effect of the adopted improvement method in the FOS. The different values of the FOS for the different stabilization methods were shown in **Figure 7**. It was observed that the factor of safety at the end of the monitoring time was 1.44 in the case of untreated soil. This value increased to 1.47 when using ordinary stone columns, the increase was insignificant this may be due to the large lateral deformation of the ordinary stone columns under the embankment toe .The factor of safety was significantly increased to 2.21 when using the ESC due to confining support provided and shears resistance offered by geosynthetic encasement, which mitigates the lateral deformation, and lateral bulging and subsequently increases the factor of safety. Looking at the slip surface as shown in

Figure 8, the slip surface was deeper (i.e., deep-seated failure) in the case of unimproved soil. Shallow slip surface with toe failure occurred at the embankment fill and it does not extend down to the treated soft soil when using ESC (i.e., the failure converted from deep-seated to surface failure). It is worth mentioning that the effect of the horizontal geosynthetic layers and BGR in general after using the encasement will have no effect on the FOS because the stability failure is dependent on the embankment material properties rather than the improved ground properties because of the surficial formed slip surface.

Figure 9 illustrates the lateral deformation (i.e., the lateral bulging) of the OSC, HRSC, ESC, ESC in addition to BGR, and V-HRSC at various depths for both the columns under the embankment center and the column near the embankment toe (i.e., Col (1) and Col (10)). The lateral deformation of Col (1) is shown in

Figure 9**a**. As predicted, the main failure mode tends to be a bulging failure, the lateral deformation of OSC approximately 3.5 times higher than those of ESC with a geotextile stiffness of 1000 kN/m. The maximum bulging of OSC was observed close to the column's surface and decreased when moving down away from the surface, this may be since the lateral earth pressure increase with depth, so the confining pressure increase finally leading to a bulging decrease, the same was observed in **[36, 37]**. The maximum deformation depth is controlled by both the loading zone and the surrounding soil's strength. This depth is approximately 1.1 * D in the current investigation, as shown in

Figure 9**a**. In comparison to OSC, the reinforced stone columns exhibited less bulging. The surface settlements are decreased when the bulging of the stone column decreases. For col 10 as indicated in **Figure** 9**b**, the main failure type was bending failure and its deformation was lateral displacement with extreme value at the surface of the column. When going deeply the lateral displacement gradually decreases and the columns remain approximately straight.
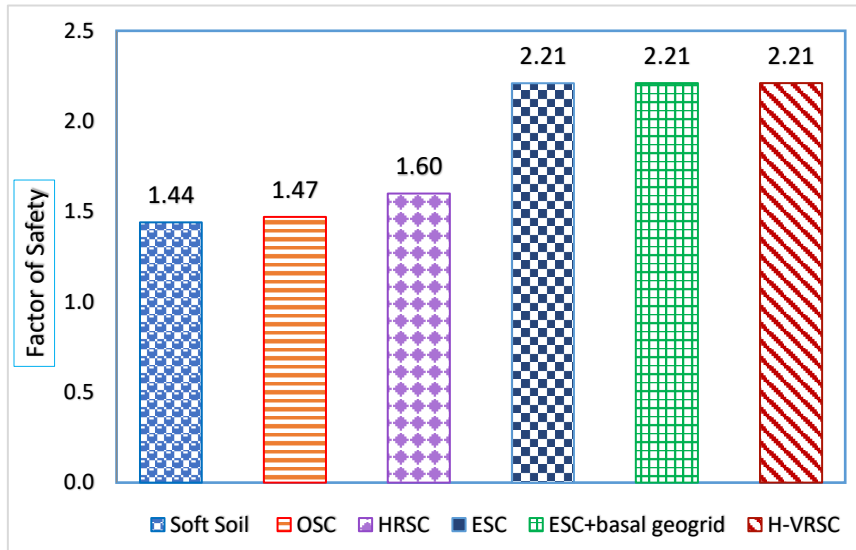
Figure 7 . Safety factors for different improvement methods

(a)- Soft soil

(b) -OSC

(c)-HRSC

(d) -ESC

(e)-ESC with BGR

(f) - V-HRSC
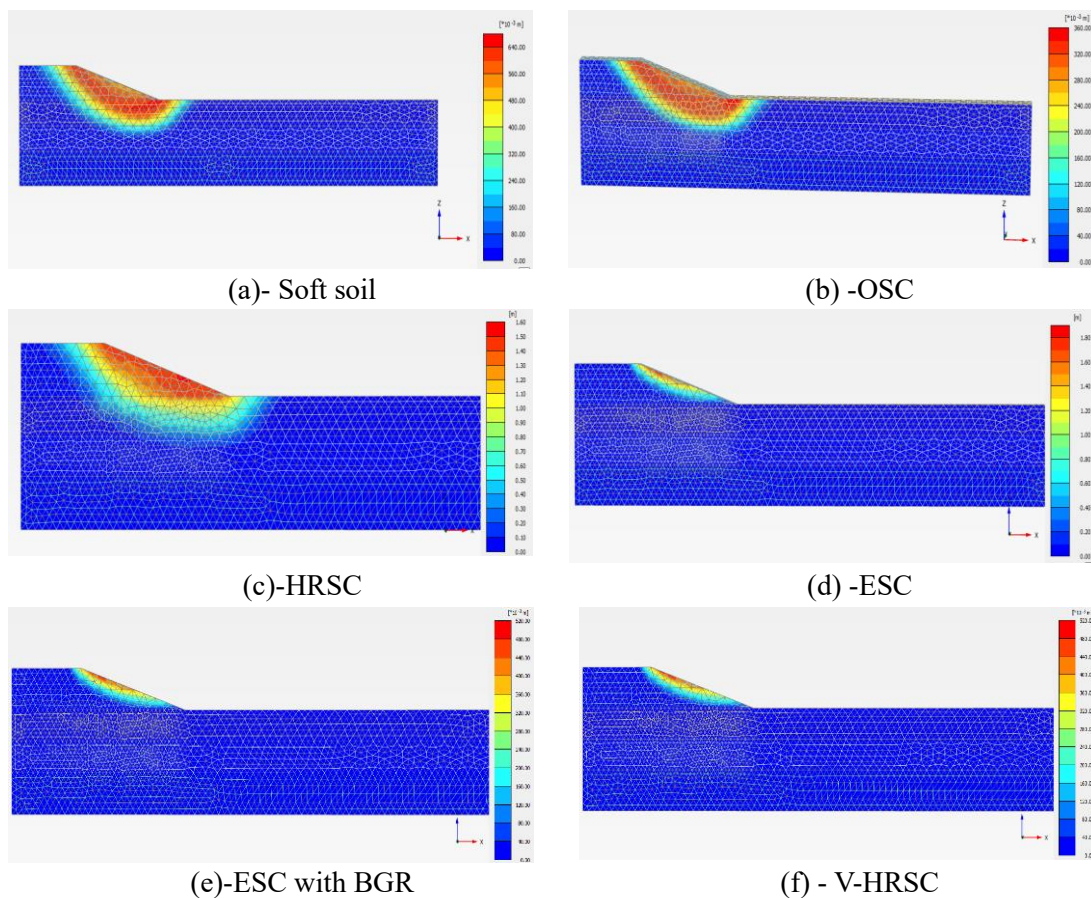
Figure 8. The development of the failure mode for varying improvement methods

(a) lateral displacement of the 1st col

(b) lateral displacement of the 10th col
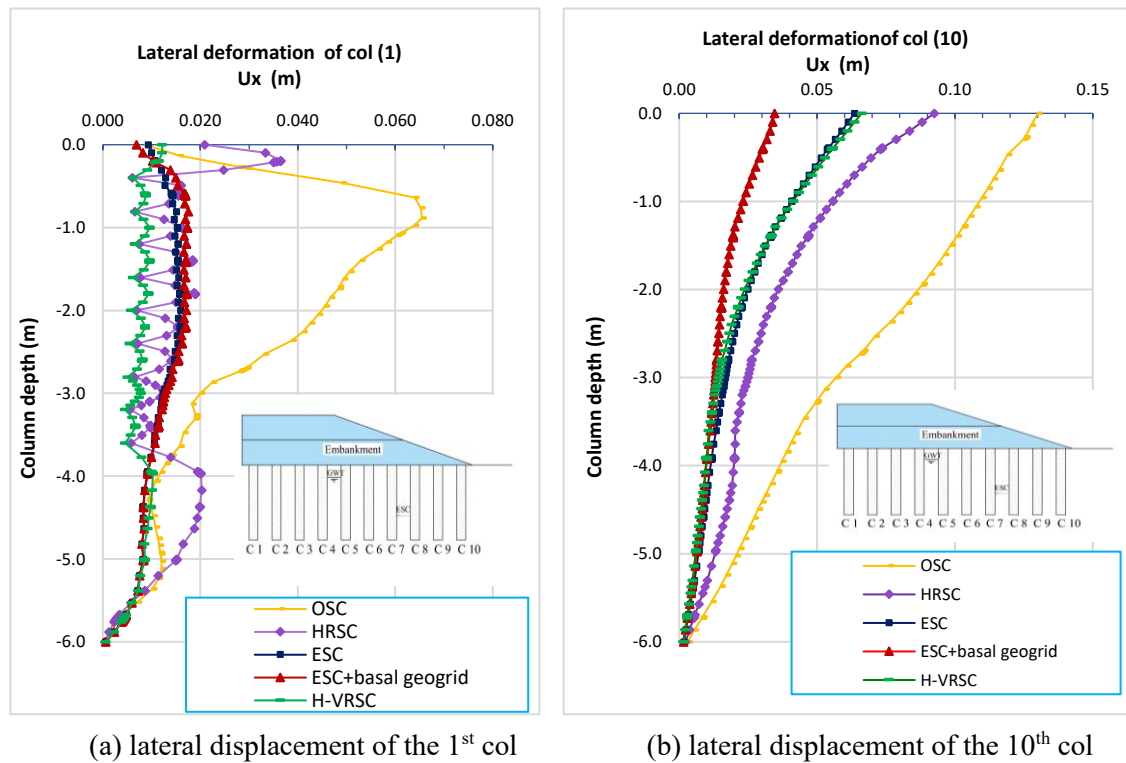
Figure 9 . (a), (b) The lateral displacement of the 1st and 10th number stone columns respectively

Figure 10a and b show the deformed shape of the embankment supported on ESC and OSC respectively. As shown in **Figure 10a**, flexural failure is the most common failure mechanism in the ESC subjected to embankment load the same was reported by **[9]**. The column's bending was induced by sliding of the embankment and the underlying soil as well as excessive lateral pressure applied to the columns. The maximum curvature of the bent columns was deeper in the columns towards the toe. The largest deformation was seen at the top of the outmost column (e.g., the column under the embankment's toe), with column deformation decreasing when the columns are close to the vicinity of the embankment's center. On the other hand, the governing failure mode of the OSC was the bulging failure and the lateral distortion as shown in **Figure 10b**.

(a)   (b)
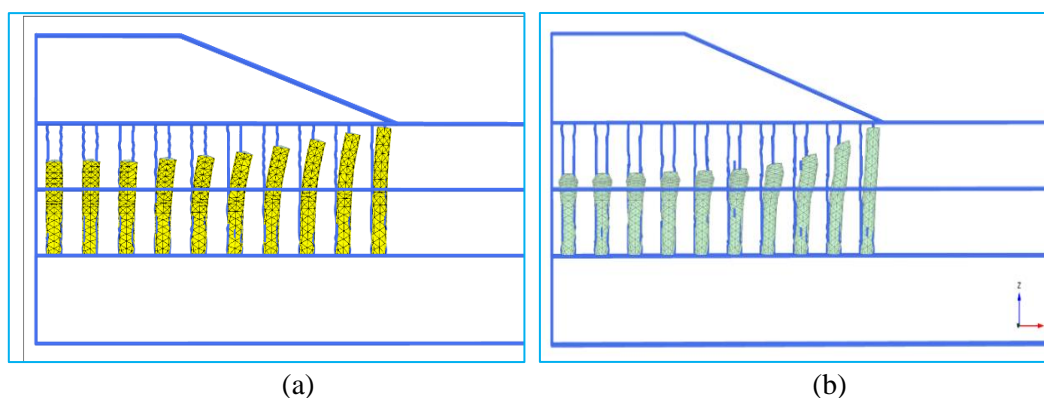
Figure 10. Deformation pattern of embankment supported by (a) ESC with a geogrid stiffness of 1000 kN/m.(b) OSC.

Figure 11 represents the development of the excess pore pressure (p_{excess} [kN/m²]) estimated at PZ1 at the mid-depth of the soft soil layers between two adjacent stone columns. The excess pore pressures

increase during embankment construction, as expected, and then progressively diminish over time. The numerical results shown in **Figure 11a** demonstrate that the excess pore water pressure generated at the end of the construction period was maximum (i.e., 30 kPa) in the case of native soil, this value significantly decreases to 11.6 kPa when using the OSC this is due to the large coefficient of permeability of the stone columns material that leads to accelerating the consolidation process in the vertical direction and consequently led to minimizing the excess pore pressure. From **Figure 11a,** we can also conclude that the time needed for dissipating excess pore water pressure to 1 kPa after the first construction stage is nearly one day and after the second construction stage is one day also when using the OSC method, compared to 23 and 25 days for the first and the second construction stages, respectively. In the case of untreated soil, which means the embankment construction period can be reduced to only 5 days instead of 60 days in this case. **Figure 11b** shows that the value of the pore pressure at the end of construction time in case of using the ESC reduced to 5.0 kPa and continued to decrease in case BGR over ESC was used until reached a minimum value (i.e., 3.47 kPa) in case using V-HRSC. The variation in the developed pore pressures could be attributed to the installation of the stone columns reduces the amount of embankment total stress transferred to the subsoil, resulting in a decrease in the maximal pore pressure.

Figure 12 illustrates the variation of the total vertical stresses (σ_{zz}) at the surface of the underlying soil along the embankment's width. The construction of stone columns eliminates stresses in the surrounding soft soils. The reduction in the total stress transferred to soft soil depends on the stone column's material stiffness and the lateral bulging of the OSC. In this study, as shown in **Figure 12,** a significant part of the embankment's loads is transported to the OSC due to the higher stiffness of the OSC compared to the surrounding soft soil. Encasing the stone columns with geosynthetics improved their stiffness, attracting more embankment loads than the OSC. This is advantageous whereas a greater portion of the embankment loads is transferred to the stone columns, reducing total stresses in the subsoil and the resulting vertical embankment deformations. This behaviour is magnified in the case of using BGR beside the ESC due to the additional stiffness given by the BGR.

(a)   (b)
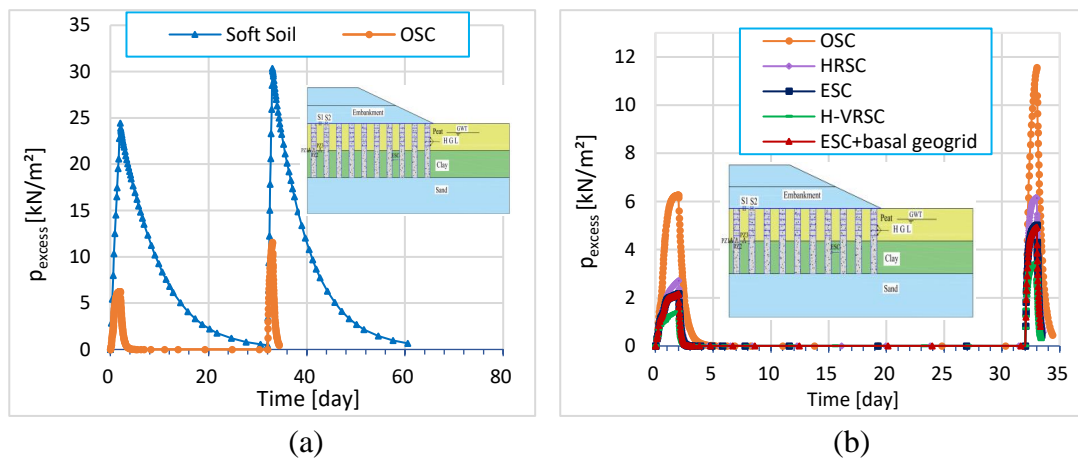
Figure 11. development of excess pore pressures versus time at PZ1
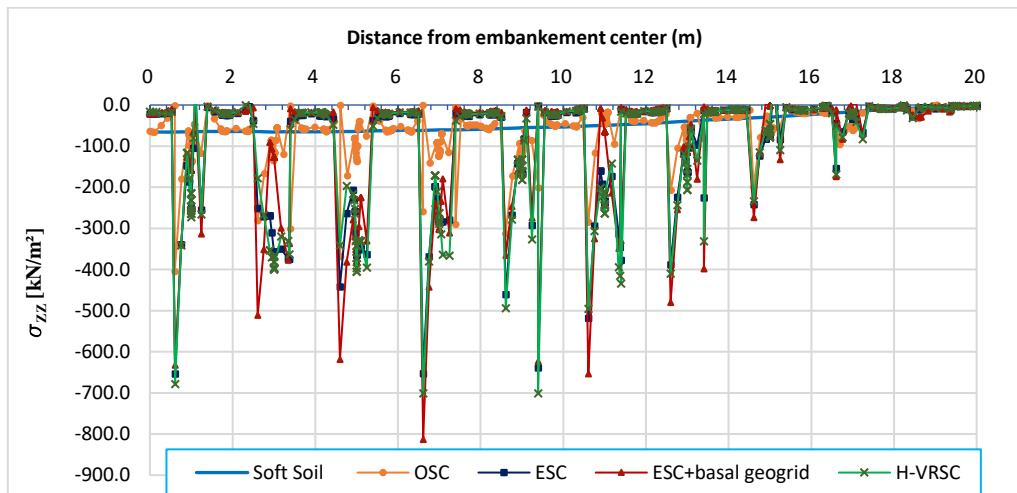
Figure 12. Vertical stresses distribution below the embankment

7. Conclusions

- Employing the ESCs to support an embankment eliminated the underlying soil settlement, increased the ratio of the stress concentration, enhanced column stiffness, and accelerated the consolidation process.
- Consolidation analyses showed that the bearing capacity of the underlying soil increases when the OSC is used to strengthen the clay because of the settlement reduction. Further increase was induced by using vertical OSC, HRSC, ESC, and ESC in combination with HGL and BGR.
- The failure mechanism of the embankment slope Transformed from a deep failure to a surface failure when using the ESC, consequently, any further improvement for the foundation soil would not affect the factor of safety.
- The factor of safety improved by approximately 11 % and 53% when using the HRSC and ESC respectively. No further increase was observed in the case of using the HGL and BGR in addition to the ESC.
- Although the OSCs do not significantly increase the embankment's safety factor, they do have a significant effect on reducing the slip surface of the embankment.
- Under embankment loading, the encased stone columns may fail by bending rather than bulging or shearing as observed in conventional stone columns. In practice, when assessing embankment stability, the ESC's bending strength should be considered.
- Ordinary stone columns reduced settlement by 49 % in comparison with unimproved soil. This value was raised to 51.5% using the HRSC. When the OSC was encased with a geosynthetic material of stiffness 1000 kN/m, the settlement reduction was 60% compared to the untreated soil and the reduction was 63% and 68% when using the basal geogrid layer in addition to the ESC and the ESC reinforced with a horizontal geosynthetic layer respectively.
- Conventional stone columns were found to be ineffective in supporting the embankment due to significant bulging caused by the absence of lateral confinement. On the other side, the reinforced stone columns either using the encasement or encasement with a horizontal reinforcement layer performed well, with a substantially less bulging and reasonable settlement, allowing for the construction of safe very high embankments.
- From the previous analysis, it was observed that from the viewpoint of the FOS the optimum value ware in the case of ESC. So, using the BGR and HGL does not affect the factor of safety.

References
1. Bayati, H. and M.H. Bagheripour, Shaking table study on liquefaction behaviour of different saturated

sands reinforced by stone columns. Marine Georesources & Geotechnology, 2019. **37**(7): p. 801-815.

2. Elsawy, M.B.J.E.J.o.G.E., Conventional and Geogrid-encased Stone Piles Improved Soft Ground under an Embankment. 2017. **22**: p. 1561-1573.

3. Jayapal, J. and K. Rajagopal, 3D Numerical Analysis of Embankments supported by Ordinary and Encased Granular Columns.

4. Kalantari, B. and Y. Tavan, 2D FEM Analysis of Stone Column-Supported Embankment and Studying the Effects of Various Parameters on Its Stability Using Cam-Clay Model.

5. Yuan, Q. and Z.-D. Cui, Two-Dimensional Numerical Analysis of the Subgrade Improved By Stone Columns in the Soft Soil Area. Marine Georesources & Geotechnology, 2016. **34**(1): p. 79-86.

6. Hasan, M., N.J.C. Samadhiya, and Geotechnics, Performance of geosynthetic-reinforced granular piles in soft clays: Model tests and numerical analysis. 2017. **87**: p. 178-187.

7. Hosseinpour, I., et al., Numerical evaluation of a granular column reinforced by geosynthetics using encasement and laminated disks. 2014. **42**(4): p. 363-373.

8. Zhang, X., et al., 3D coupled mechanical and hydraulic modeling of geosynthetic encased stone column-supported embankment over soft clay. 2021. **39**(11): p. 1285-1295.

9. Chen, J.-F., et al., Failure mechanism of geosynthetic-encased stone columns in soft soils under embankment. 2015. **43**(5): p. 424-431.

10. Abusharar, S.W. and J. Han, Two-dimensional deep-seated slope stability analysis of embankments over stone column-improved soft clay. Engineering Geology, 2011. **120**(1): p. 103-110.

11. Dar, L.A. and M.Y.J.T.I.G. Shah, Deep-seated slope stability analysis and development of simplistic FOS evaluation models for stone column-supported embankments. 2021. **8**(2): p. 203-227.

12. Jayapal, J. and K. Rajagopal. Numerical Study of Embankments Supported by Ordinary and Encased Granular Columns in Peat. in Advances in Computer Methods and Geomechanics: IACMAG Symposium 2019 Volume 2. 2020. Springer Nature.

13. Ng, K., Y.J.J.o.E.S. Chew, and Technology, Slope stability analysis of embankment over stone column improved ground. 2019. **14**(6): p. 3582-3596.

14. Pandey, B., S. Rajesh, and S. Chandra, 3-D Finite Element Study of Embankment Resting on Soft Soil Reinforced with Encased Stone Column, in Problematic Soils and Geoenvironmental Concerns. 2021, Springer. p. 451-465.

15. Yoo, C. and S.-B.J.G.I. Kim, Numerical modeling of geosynthetic-encased stone column-reinforced ground. 2009. **16**(3): p. 116-126.

16. Zheng, G., et al., Influence of geosynthetic reinforcement on the stability of an embankment with rigid columns embedded in an inclined underlying stratum. 2021. **49**(1): p. 180-187.

17. Zhou, Y., et al., Evaluation of geosynthetic-encased column-supported embankments with emphasis on penetration of column toe. 2021. **132**: p. 104039.

18. Han, J., et al., Evaluation of deep-seated slope stability of embankments over deep mixed foundations, in GeoSupport 2004: Drilled Shafts, Micropiling, Deep Mixing, Remedial Methods, and Specialty Foundation Systems. 2004. p. 945-954.

19. Manual, P.D.C.V.-T., 2021.

20. Brinkgreve, R., W. Broere, and D.J.T.N. Waterman, Plaxis, Finite element code for soil and rock analyses, users manual. 2006.

21. Phutthananon, C., et al., Numerical study of the deformation performance and failure mechanisms of TDM pile-supported embankments. 2021. **30**: p. 100623.

22. Liu, K.W. and R.K. Rowe, Performance of reinforced, DMM column-supported embankment considering reinforcement viscosity and subsoil's decreasing hydraulic conductivity. Computers and Geotechnics, 2016. **71**: p. 147-158.

23. Jamsawang, P., et al., Three-dimensional numerical analysis of a DCM column-supported highway embankment. 2016. **72**: p. 42-56.

24. Wang, A. and D. Zhang, Lateral Response and Failure Mechanisms of Rigid Piles in Soft Soils Under Geosynthetic-Reinforced Embankment. International Journal of Civil Engineering, 2020. **18**(2): p. 169-184.

25. Dar, L.A., M.Y.J.G. Shah, and G. Engineering, Three dimensional numerical study on behavior of geosynthetic encased stone column placed in soft soil. 2021. **39**(3): p. 1901-1922.

26. Lo, S., et al., Geosynthetic-encased stone columns in soft clay: a numerical study. 2010. **28**(3): p. 292-302.

27. Naseer, S., et al., Laboratory and numerical based analysis of floating sand columns in clayey soil. 2019. **10**(1): p. 1-16.

28. Huang, B., et al., Numerical study of reinforced soil segmental walls using three different constitutive soil models. 2009. **135**(10): p. 1486-1498.

29. Leshchinsky, D. and C.J.G.I. Vulova, Numerical investigation of the effects of geosynthetic spacing on failure mechanisms in MSE block walls. 2001. **8**(4): p. 343-365.

30. Hosseinpour, I., et al., A comparative study for the performance of encased granular columns. 2019. **11**(2): p. 379-388.

31. Parsa-Pajouh, A., et al., Trial embankment analysis to predict smear zone characteristics induced by prefabricated vertical drain installation. 2014. **32**(5): p. 1187-1210.

32. Schanz, T., P. Vermeer, and P.G. Bonnier, The hardening soil model: formulation and verification, in Beyond 2000 in computational geotechnics. 2019, Routledge. p. 281-296.

33. Brinkgreve, R.B., et al., Plaxis material models manual. 2020.

34. Almeida, M. and M. Marques, Design and Performance of Embankments on Very Soft Soils. 2013.

35. Jeong, S., et al., Time-dependent behavior of pile groups by staged construction of an adjacent embankment on soft clay. 2004. **41**(4): p. 644-656.

36. Debbabi, I.E., et al., Numerical modeling of encased stone columns supporting embankments on sabkha soil. 2020. **6**(8): p. 1593-1608.

37. Vibhoosha, M., A. Bhasi, and S. Nayak, Effect of geosynthetic stiffness on the behaviour of encased stone columns installed in lithomargic clay, in Advances in Computer Methods and Geomechanics. 2020, Springer. p. 197-207.

دراسة عددية لسلوك الجسور المبنية على تربة لينة محسنة بالأعمدة الحبيبية العادية والاعمدة المقواة بالمواد البوليميرية الاصطناعية

الملخص العربي

قد تخضع المنشآت المبنية على التربة الطينية الضعيفة لقيم كبيرة من الهبوط، وعدم الاستقرار، وكذلك حدوث إزاحة جانبية كبيرة لطبقة التربة الرخوة. تعمل الأعمدة الحجرية العادية والأعمدة الحبيبية المقواة بالمواد البوليميرية الاصطناعية على تقليل قيم الهبوط وتحسين قدرة تحمل تربة الاساس الضعيفة. في هذا البحث تم استخدام برنامج متخصص في حل المسائل الجيوتقنية لدراسة سلوك الجسور المقامة على التربة الطينية الضعيفة جدا المحسنة باستخدام الأعمدة الحبيبية على فترة زمنية كبيرة. يعتبر تغليف العمود المكون من المواد الحبيبية باستخدام اغلفة من المواد البوليميرية الصناعية هو النوع الأكثر شيوعًا في تسليح وتدعيم الاعمدة الحبيبية؛ ومع ذلك، تم في هذا البحث اقتراح استخدام طبقات الجيوتكتسيل الافقية داخل الاعمدة الحبيبية. حيث تم استخدام المواد البوليمرية الاصطناعية (الجيوتكستيل) لتقوية الاعمدة الحبيبية في شكل تغليف عمودي، وطبقات أفقية، وتقوية العمود بتغليفه بمواد البوليمر مع وضع طبقات جيوتكستيل افقية داخله على مسافات معينة في نفس الوقت. تم عمل دراسة مقارنة في هذا البحث بين هذه الأشكال المختلفة لتقوية الاعمدة الحبيبية المؤسسة في التربة الطينية وتأثيرها على سلوك الجسر. أظهرت نتائج البحث أن استخدام العمود الحجري المغلف والأعمدة الحجرية المقواة رأسيا وافقيا قد أدى إلى تحسن كبير في التشوه الجانبي للعمود على كامل طوله، وتولد وتبديد ضغط الماء البيني الزائد، والهبوط. لوحظ ايضا زيادة في معامل الأمان ضد الانزلاق الجانبي للجسر بنسبة ٥٣٪ باستخدام الاعمدة المغلفة بمواد البوليمر في تحسين التربة مقارنة بالتربة غير المعالجة. استخدام طبقة من الجيوجريد أسفل جسم الجسر او استخدام الطبقات الافقية بعد تغليف الأعمدة الحبيبية ليس لهما تأثير على معامل الأمان حيث تحول سطح الانزلاق من سطح عميق يمر بالتربة الضعيفة إلى سطحي يعتمد فقط على خصائص مادة جسم الجسر.